Cellular automaton simulation of pedestrian counter flow considering the surrounding environment

Y. F. Yu and W. G. Song*
State Key Laboratory of Fire Science, University of Science and Technology of China, Hefei, Anhui, 230027, People's Republic of China

(Received 24 November 2006; revised manuscript received 26 January 2007; published 20 April 2007)

This paper presents a cellular automaton model without step back to simulate the pedestrian counter flow in a channel. The consideration of the surrounding environment when people make judgments on moving directions is added to a random walker model also without step back. Two types of walkers: the right walkers going to the right and the left walkers going to the left are taken into account. The characteristics of counterflow are clarified. Influences of the different interaction radius values and system sizes on movement are studied. Phase transition from free moving to jamming is observed with the increase of entrance density. It is found that the critical entrance density p_c at the transition point does not depend on the system size when the interaction radius value is large. Simulation results are represented as a comparison with the random walker model.

DOI: 10.1103/PhysRevE.75.046112 PACS number(s): 89.40.−a, 05.50.+q, 05.70.Fh, 05.90.+m

I. INTRODUCTION

Recently, the cellular automaton (CA) model has been frequently and extensively used in pedestrian evacuation [1–6,8–13]. Instead of making detailed assumptions about pedestrians' behavior, static floor field (SFF) and dynamic floor field (DFF) are used to reproduce many collective effects [1–5]. SFF does not change in time. It is related with the surrounding geometry, i.e., the walking ground where the evacuation takes place. The distance from a cell on the lattice in the CA model to an exit door is usually stored in its relative SFF value, and that information tells the pedestrian on the cell where the exit door is and how to reach it from his current position and then to escape successfully. While DFF, on the other side, changes almost every simulation update step during the whole evacuation, including diffusion and decay. Inspired from the idea of chemotaxis, the concept DFF represents a virtual trace left by moving pedestrians. Subsequent pedestrians follow the preceding pedestrians' footprints by inspecting the information (i.e., DFF) left [1,2]. It reflects in a respect how the human trail evolves in the real world [6].

Kirchner *et al.* [3] investigated the role of conflicts in pedestrian traffic, extended CA model, and introduced a friction parameter μ. It is found that conflict effects are not an unexpected artifact of the parallel update procedure, but are important for an exact description of real evacuation dynamics. Henein and White added another important element: local pushing, by introducing a force floor field [4]. Then three kinds of forces between one pedestrian and another, and those between pedestrians and walls, are taken into account by Song *et al.* [5]. All these forces, i.e., repulsion, friction, and attraction, are basic reasons for complex behaviors to emerge from evacuation. Helbing *et al.* [7] proposed a many-particle-inspired theory to study in a different way the coordination problems resulting from the competition of too many entities for little space.

On the other hand, the CA model is extended by using the transition (hopping) probability scheme [8–13]. Each pedestrian on a cell moves into adjacent cells with probabilities. Phase transition from free moving to perfect stop of counterflow in a channel is simulated [8]. The dependence of the jamming transition on system size [8,10], drift strength [8], partition line [9], back stepping [10], and traffic rules [8,13] have been studied. For evacuations in such places as smoky rooms and corridors with low ceilings, pedestrians involved move out on all fours. Experiments are carried out and models are developed to simulate slender particles on a square lattice [11,12] for these situations. Weng *et al.* [13] simulated counterflow of pedestrians with different velocities. Phase transition among freely moving phase, lane formation phase, and perfectly stopped phase are also observed.

However, the transition probability schemes in these research works are almost of the same pattern: the pedestrian can move forward, backward, right, left or stay. If it is a model without back step, the movement in the backward direction is restricted. All these hopping probabilities result from the adjacent cells' status in the corresponding direction. Usually, only four or three (in the case of no back steps) adjacent cells' status are taken into account for a pedestrian to decide which way to go. That is a little different from the way we make judgements during real pedestrian traffic, in which case not only the nearest neighbor cells' status mentioned above are considered, but all around cells (e.g., cells in corner directions like left-forward and right-forward, or cells that are three cells away from the current cell) are taken into consideration. Kirchner *et al.* [14] have also investigated the influence beyond nearest neighbor interactions by increasing the maximal walking speed $v_{\max}$ from the original 1 cell per update step. Basically speaking, the widening of the visible area of pedestrians should not be due to or at least not only due to a faster movement. It is an inherent ability of pedestrians. With whatever speed they walk, even when $v_{\max}=1$ as in the random walker model, pedestrians should still be aware of the influence of others beyond their neighborhood.

In this paper, we introduce a parameter called interaction radius to represent the considering of the surrounding envi-

*Electronic address: wgsong@ustc.edu.cn

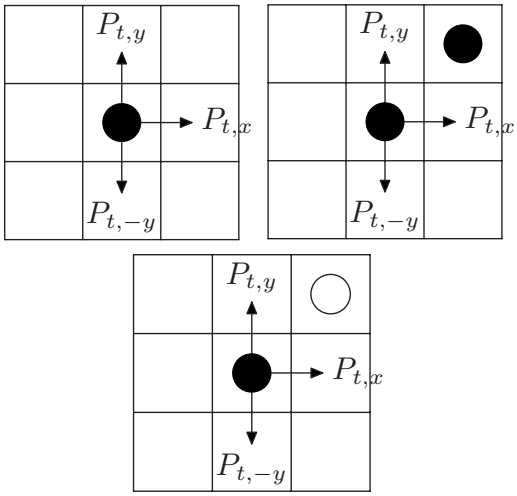

FIG. 1. Transition probability configurations of the right walker going to the right, indicated by the full circle, while the open circle indicates the left walker going to the left.

ronment of pedestrians during movement. To clarify how it improves the movement process, we compare it with a random walker model without step back which has a very simple transition probability scheme.

II. MODEL

The random walker model without step back can be seen as a simple special case of the model used in Ref. [8] with heading drift $D=0$. The excluded-volume effect is taken into account, which means one cell can only hold one particle. The transition probability matrix of the random walker model without step back can be described as follows:

$$p_m = \frac{1}{n}, \tag{1}$$

where m means possible moving directions: up, down, left or right, p_m is the transition probability of the corresponding direction, and n is the number of moving directions available.

So without any particles on his adjacent cells in Fig. 1, the right walker (going to the right, indicated by the full circle) has three moving directions available: up, down, right. Each direction is equal to be chosen with a probability of 1/3.

But what if there is a walker on his up-right-hand side as shown in Fig. 1(b)? It should have some impact on his transition probability matrix, and eventually influence the movement behavior of pedestrians. Or maybe, it is not a right walker as himself he encounters but a left walker (going to the left, indicated by the empty circle) as shown in Fig. 1(c)? All these configurations make no difference to the transition probability matrix in recent use of CA models, which have been improperly ignored and have not been well studied.

We introduce the interaction radius (R_i) parameter to consider situations like Fig. 1(b) and Fig. 1(c). Particles make judgements after collecting information on an area within R_i cells around his current position. Take $R_i=1$ as an example,

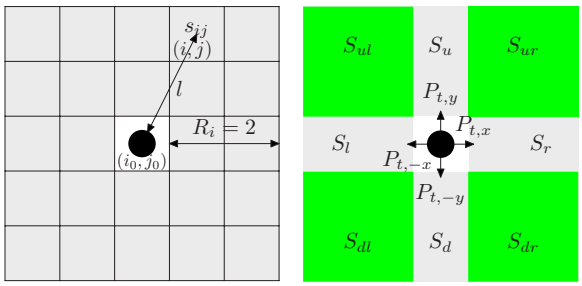

FIG. 2. (Color online) Illustration of interaction radius and calculation of various S values.

particles will look at $8[=(R_i\times 2+1)^2-1]$ cells, i.e., all the cells around, except for the central one in Fig. 1(a), before he decides which way to move.

In the case of $R_i=2$, 24 cells are taken into account [Fig. 2(a)]. As for the pedestrian in the center (we call him the central pedestrian or the pedestrian under consideration) of Fig. 2(a), he collects the information s_{ij} of all the gray cells, which reflects the impact of the cell at position (i,j) (denoted as c_{ij} in the following context) on his current position (i_0,j_0),

$$s_{ij} = L_{ij}O_{ij}. \tag{2}$$

L_{ij} represents the dependence of s_{ij} on the distance l between c_{ij} and the central cell. And O_{ij} represents the relation between s_{ij} and the occupancy information of c_{ij}: whether it is occupied and occupied by which kind of particle.

The interaction between two pedestrians over a distance decreases with the increase of their distance. When the distance between them is small, changes of the distance do not result in much difference on the interaction, while if the distance gets bigger and exceeds some critical value, the interaction decreases sharply with the increase of the distance. Based on this and Refs. [15,16], we calculate L_{ij} as follows to make simulation rules simple, and l_c is the critical value of distance, which is valued as four cells in our simulation,

$$L_{ij} = \begin{cases} 1, & l < l_c, \\ 1/l, & l \geqslant l_c, \end{cases} \quad \text{where } l = |i-i_0| + |j-j_0|. \tag{3}$$

O_{ij} is obtained as shown in formula (4). This means we do not distinguish whether the cell is occupied by a left walker or a right walker,

$$O_{ij} = \begin{cases} 0, & c_{ij} \text{ is empty}, \\ 1, & c_{ij} \text{ is occupied}. \end{cases} \tag{4}$$

A new O_{ij} function [formula (5)] that distinguishes occupancy information is also used in our study and results are shown as a comparison. This represents that the interaction among pedestrians with different speeds is larger than that among pedestrians with the same speed,

$$O_{ij} = \begin{cases} 0, & c_{ij} \text{ is empty,} \\ 1, & c_{ij} \text{ is occupied by a pedestrian in the same group as the central pedestrian,} \\ 2, & c_{ij} \text{ is occupied by a pedestrian in the other group.} \end{cases} \quad (5)$$

Every walker calculates the s_{ij} information of cells within the interaction radius. S_{ul} indicates the sum of s_{ij} of cells on the up-left-hand side of the pedestrian under consideration [the full circle in the center of Fig. 2(b)]. And $S_{ur}, S_{dl}, S_{dr}, S_u, S_d, S_l, S_r$ correspond to the up-right-hand, down-left-hand, down-right-hand, directly up, directly down, directly left, directly right-hand side cells, respectively. Since particles are only able to move left, right, up, and down on the lattice, $S_{ul}, S_{ur}, S_{dl}, S_{dr}$ are projected and added their influence on these directions. Because pedestrians prefer to move forward, the probabilities of moving sideways are much more impressionable than the probability of moving directly forward under the influence from corner directions. Thus to make rules simple, we just consider the influence of corner directions on the probabilities of moving sideways. S_u and S_d are revised as follows to reflect that influence:

$$S_u = S_u^0 + 0.5(S_{ul} + S_{ur}),$$

$$S_d = S_d^0 + 0.5(S_{dl} + S_{dr}). \quad (6)$$

After all these are done, S_u, S_d, S_l, S_r are used to revise the transition probabilities in formula (1) as follows:

$$P_m = N p_m T(S_m) = N \frac{1}{n} \frac{1}{1 + S_m},$$

$$\text{with normalization,} \quad N = \left(\sum_m P_m \right)^{-1}. \quad (7)$$

Here, the T function is used to reflect the influence of S values on moving probabilities, which is usually a monotone decreasing function. In our simulation we choose $T(S_m) = 1/(1+S_m)$ which informs: if $S_m = 0$, there is no influence from the surrounding environment and no need to revise p_m, while in other cases where $S_m > 0$, it always decreases the transition probability in the corresponding direction and increases the transition probabilities of other directions after the normalization of the transition probability matrix.

III. SIMULATION AND RESULTS

Figure 3 shows the schematic illustration of the pedestrian counterflow in a channel in our model. Initially, there are no walkers in the channel. The right (left) walkers are randomly distributed on the left (right) boundary with an entrance density p_l (p_r). All walkers are numbered randomly from 1 to N (total number of walkers within the channel, including boundaries), which guarantees the upcoming sequential update to work like a parallel (synchronous) update. Following the rules mentioned in the preceding section, the numbered walkers are updated in order. If the right (left) walkers reach the right (left) boundary, they are removed from the channel. After all these points are done, one update step is completed. In the next time step, a number of new walkers are generated on random positions on boundaries, which ensures that the entrance density on the left-hand (right-hand) boundary remains p_l (p_r). The above procedure is repeated.

We carry out simulations on the counterflow in a $W \times L$ channel without back steps. For different total entrance density $p(\equiv p_l + p_r)$, the mean velocity $\langle v \rangle$ and the occupancy ρ are checked. The mean velocity $\langle v \rangle$ at one update step is defined as the number of walkers who choose to move forward divided by the total number of walkers in the channel. The occupancy ρ is self-explainable, which is defined as the total number of walkers in the channel divided by the channel area $(W \times L)$.

For each simulation, 10 000 time steps are carried out, and the value of $\langle v \rangle$ and ρ are computed according to the last 4000 time steps averaged over 10 runs. O_{ij} in formula (4) is used, and results of simulation using the new O_{ij} in formula (5) are shown as a comparison at the end of this section.

First we give the simulation results derived from the random walker model without step back, with which results of our model are compared. Figure 4(a) shows the plot of the mean velocity $\langle v \rangle$ against the total entrance density p for $W = 10$, 20, 50, 80, and 100 in the case of $L = 100$. As we can see, the mean velocity decreases with increasing p when p is small. And when p gets larger than the critical entrance density (indicated as p_c), $\langle v \rangle$ goes down sharply to zero. This indicates the phase transition from free moving to jamming and perfect stop. Figure 4(b) shows the plot of the occupancy ρ against the total entrance density p for the same simulation results as those in Fig. 4(a). The occupancy increases gradu-

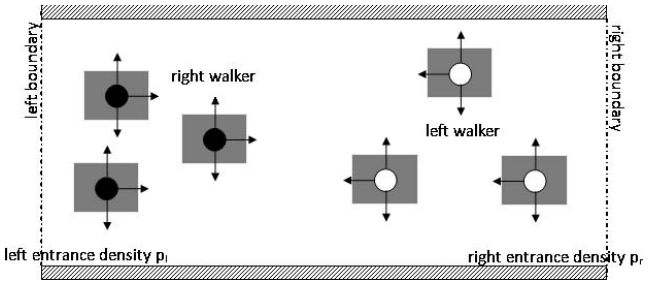

FIG. 3. Schematic illustration of the pedestrian counter flow in a channel in our model. The top and bottom sides of the channel are walls. The left-hand and right-hand sides are open boundaries. The right (left) walker going to the right (left) is indicated by the full (open) circle, and comes into the channel from the left (right) boundary with a constant entrance density p_l (p_r). Arrows indicate possible moving directions of the two groups. Gray field around the circle indicates the interaction radius.

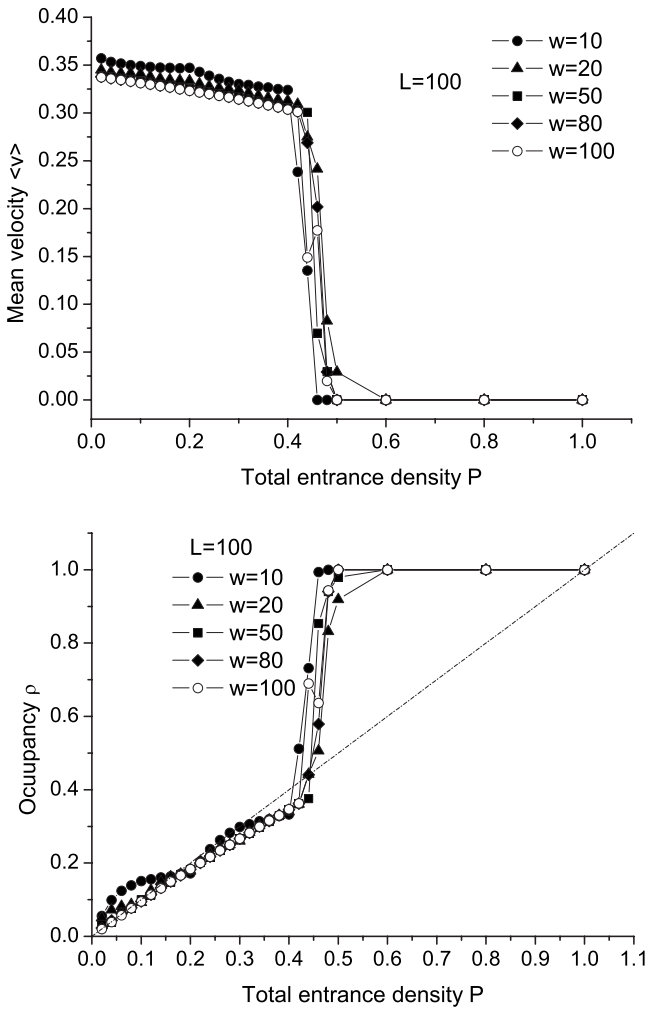

FIG. 4. Plots of the mean velocity $\langle v \rangle$ and the occupancy ρ against the total entrance density p for $W=10$, 20, 50, 80, and 100 in the random walker model where $L=100$.

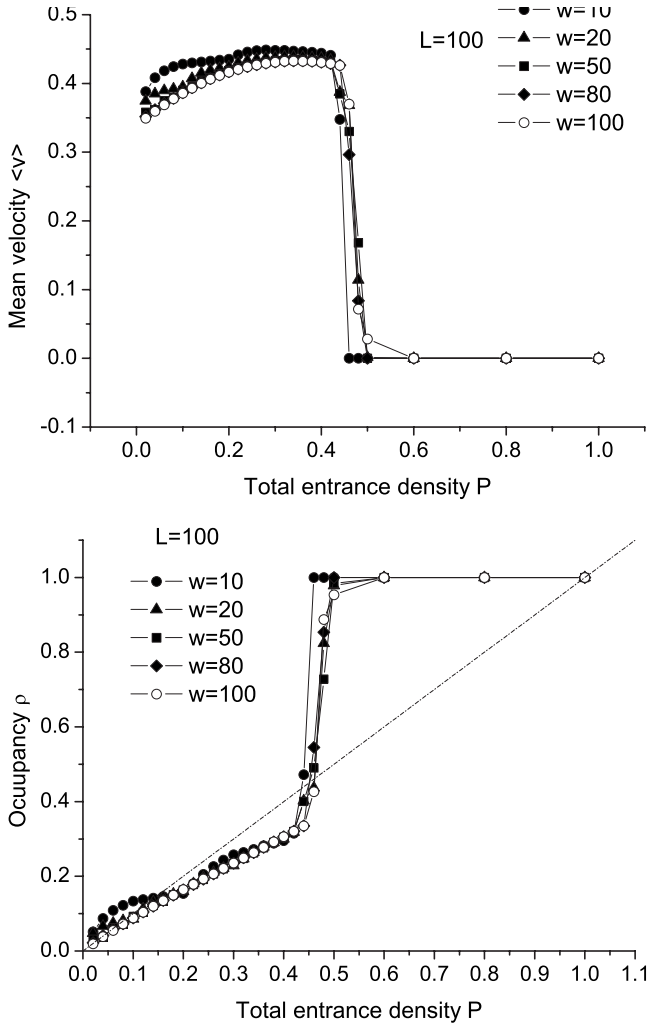

FIG. 5. Plots of the mean velocity $\langle v \rangle$ and the occupancy ρ against the total entrance density p for $W=10$, 20, 50, 80, and 100 in our CA model where $L=100$ and $R_i=2$.

ally as increasing p when p is small. And it goes up sharply to one when p gets larger than p_c. Notice that the $[0,p_c]$ part of the curve ρ-p is below the dashed-dotted line $\rho=p$. This means that even at the free moving state, the interaction among pedestrians in movement still plays a role to make the pedestrian density in the channel smaller than the total entrance density from a long time view.

Figure 5 shows the plots of the mean velocity $\langle v \rangle$ and the occupancy ρ against the total entrance density p for $W=10$, 20, 50, 80, and 100 in our CA model considering the surrounding environment where $L=100$ and $R_i=2$. Roughly the same trends are derived, except for some interesting differences. If p are very small, there is not many particles in the system. Considering the surrounding environment almost makes no difference with simulation than without this consideration. But when p gets a little larger, the number of particles in the system increases. The difference of considering the environment comes out. Unlike Fig. 4(a), with the increase of entrance density p, the mean velocity goes up a while and then slows down and finally drops sharply to zero after p exceeds p_c [Fig. 5(a)]. And the mean velocity of pedestrians in free moving is larger than that in Fig. 4(a). It is because after considering the surrounding environment, a pedestrian adjusts his transition probabilities into a pattern that is more valuable and helpful to an efficient movement. It makes him encounter less obstacles and lowers the probability of getting stuck.

Figure 6 shows the plots of the mean velocity $\langle v \rangle$ and the occupancy ρ against the total entrance density p when $R_i=5$. Two things should be noticed. One is the deviation of curve ρ-p at the free moving state from the dashed-dotted line $\rho=p$ becomes larger from Fig. 4 to Fig. 6. Take $W=100$ as an example, when $p=0.42$, the occupancy ρ is 0.3625 in the random walker model, 0.3205 in the case of $R_i=2$, and 0.3135 when $R_i=5$. When R_i becomes larger, pedestrians get more information about the surrounding environment, and they do not waste their time on idle work of wandering. Therefore the mean velocity $\langle v \rangle$ at the free moving state in Fig. 6 is larger than that in Figs. 5 and 4. The other thing is from Fig. 4 to Fig. 5 and then to Fig. 6, the curves with different W values are getting closer. Especially for the $p \in [0.2,0.4]$ part of the free moving state, curves almost overlap with each other when $R_i=5$. That means if

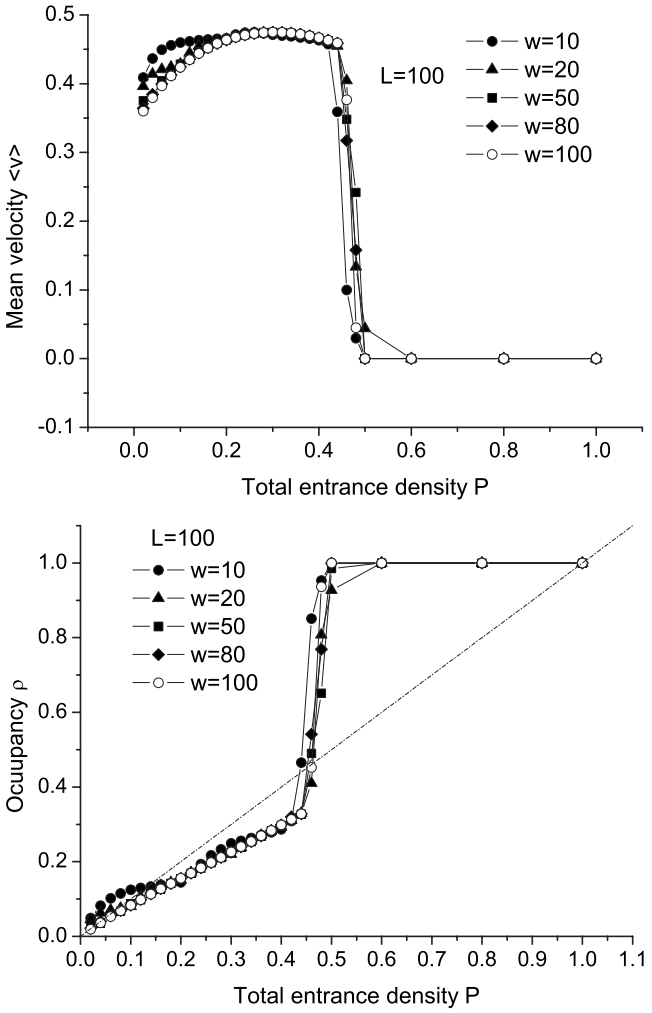

FIG. 6. Plots of the mean velocity $\langle v \rangle$ and the occupancy ρ against the total entrance density p for $W=10$, 20, 50, 80, and 100 in our CA model where $L=100$ and $R_i=5$.

pedestrians in movement collect enough information about the outer environment, the width of the channel becomes less important to the movement process.

Figure 7 shows the plots of the critical total entrance density p_c against the inverse $1/W$ of W. In all three cases, when the width W is larger than 80, the critical density p reaches to a constant. It is found that the jamming transition does not depend on the system size, especially when the interaction radius value is large. As shown in Fig. 7(c), when the width W is larger than 20, the critical density p becomes constant. In our simulation, considering the surrounding environment does not effect much on p_c, although due to the reason before, the average p_c increases from 0.43 to 0.45 from Fig. 7(a) to Fig. 7(c).

The entrance density on the left-hand boundary p_l in all simulations above are equal to the entrance density on the right-hand boundary p_r. What if the entrance densities on both boundaries are nonsymmetrical? We study the dependence of $\langle v \rangle$ and ρ on the fraction c. c is defined as the ratio of p_l to the total entrance density p. We run simulations on the case $W=50$, $L=100$, $p_l=cp$, $p_r=(1-c)p$ for different c values: 1/2, 1/3, 1/4, 1/5, 1/8, and 1/10, using the random

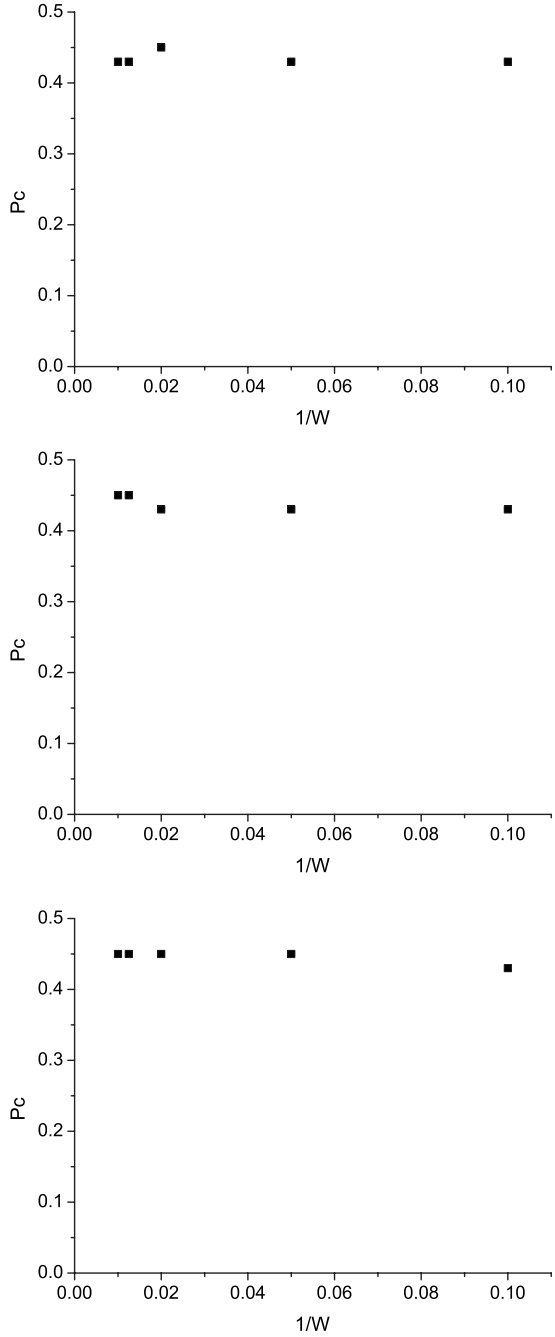

FIG. 7. Plots of the critical total entrance density p_c against the inverse $1/W$ of W for $L=100$ in the random walker model and in our CA model with $R_i=2$ and $R_i=5$.

walker model, and our model with $R_i=2$ and $R_i=5$. Results are shown in Figs. 8 and 9. It is found that at the free moving state, changes of the fraction c influence little on the mean velocity $\langle v \rangle$ and the occupancy ρ. While at the early jamming state ($p \in [0.4, 0.6]$), the more asymmetrical the entrance densities on both boundaries are, the more beneficial it is to the movement process. To the extreme, when $c=0$ (well, $c=1$ is the same), there is only one group of pedestrians in the channel. And it is more difficult to get into the perfect stop phase.

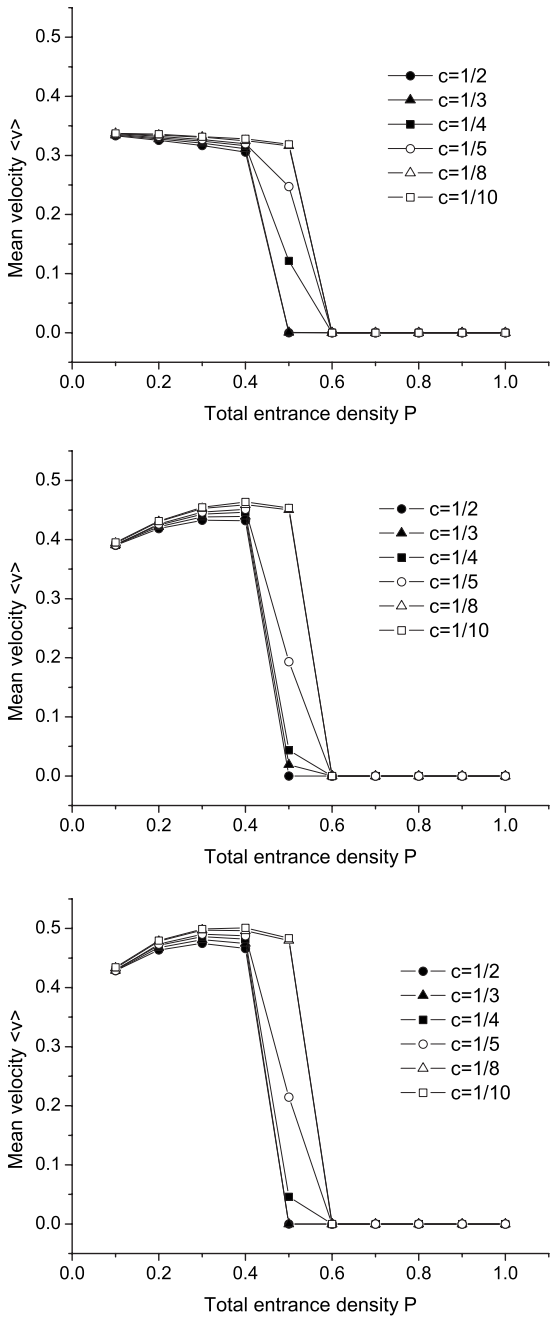

FIG. 8. Plots of the mean velocity $\langle v \rangle$ against the total entrance density p for different fractions $c=1/2$, $1/3$, $1/4$, $1/5$, $1/8$, and $1/10$, where $W=50$, $L=100$, $pl=cp$, and $pr=(1-c)p$ in the random walker model and in our CA model with $R_i=2$ and $R_i=5$.

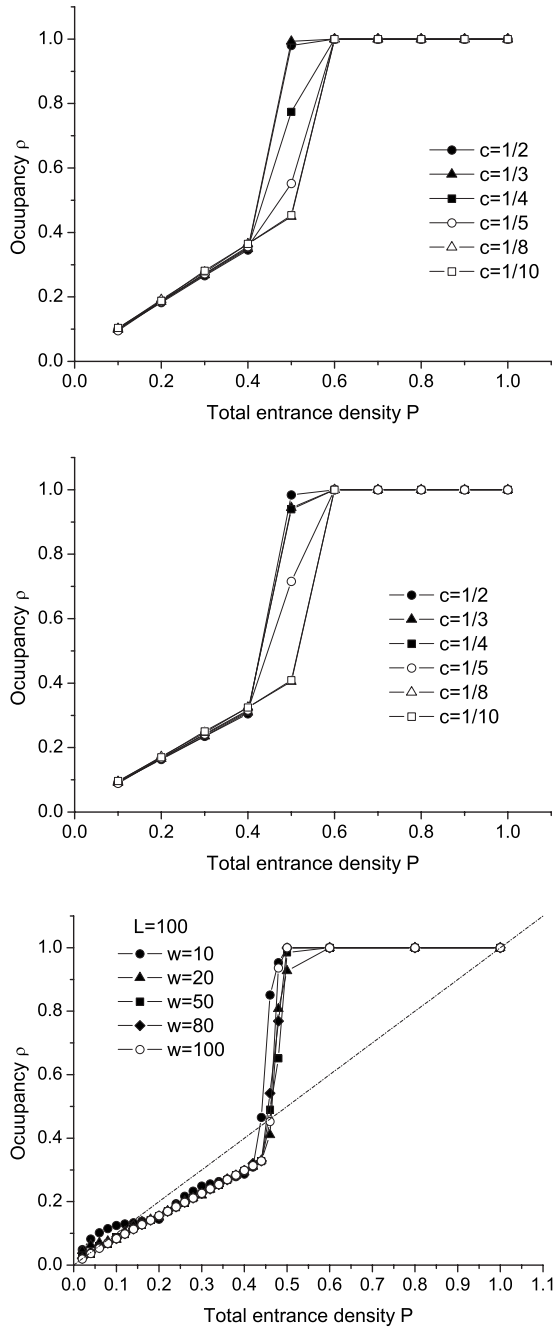

FIG. 9. Plots of the occupancy ρ against the total entrance density p for different fractions $c=1/2$, $1/3$, $1/4$, $1/5$, $1/8$, and $1/10$, where $W=50$, $L=100$, $pl=cp$, and $pr=(1-c)p$ in the random walker model and in our CA model with $R_i=2$ and $R_i=5$.

The tendency of how the results change against the fraction c is more clear in Fig. 10. We run simulations on the case $L=100$, $W=50$, $P=0.5$ with different c values using the random walker model and our model with $R_i=2$ and 5. It is also shown that c affects the movement process at the early jamming state more than at the free moving state or at the perfect stop state. This tendency and the slopes of these three curves are similar. Therefore, how the asymmetry of the entrance densities on both boundaries influences the movement process depends little on the interaction radius.

Figure 11 shows plots of the mean velocity $\langle v \rangle$ and the occupancy ρ against the total entrance density p for $L=100$, $W=20$ and 50, $R_i=2$ and 5 using different O_{ij} functions. As mentioned at the beginning of this section, here we use a new O_{ij} function in formula (5) for our model to distinguish the occupancy information of c_{ij}. It is found that with the same simulation conditions, pedestrians using the new movement strategy move faster than before, while the occupancy ρ does not change much.

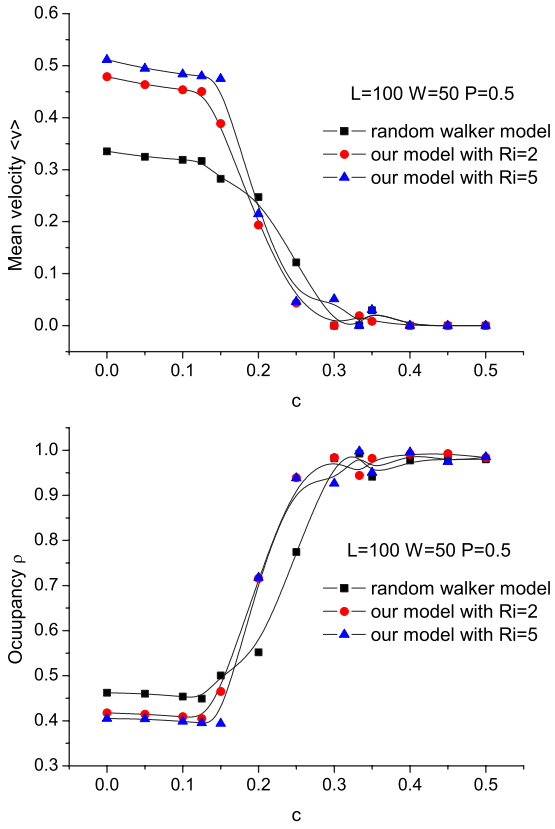

FIG. 10. (Color online) Plots of the mean velocity $\langle v \rangle$ and the occupancy ρ against the fraction c for $L=100$, $W=50$, and $P=0.5$ in the random walker model and our model with $R_i=2$ and 5.

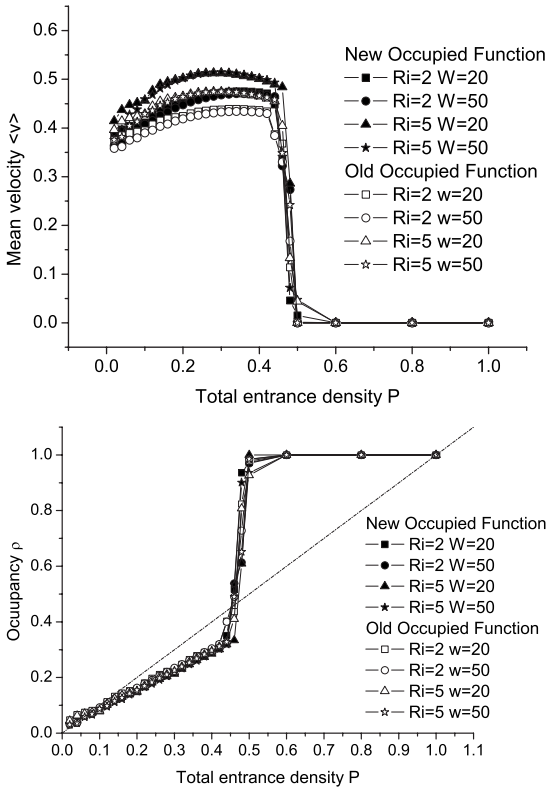

FIG. 11. Plots of the mean velocity $\langle v \rangle$ and the occupancy ρ against the total entrance density p for $L=100$, $W=20$ and 50, $R_i=2$ and 5 using different O_{ij} functions.

IV. CONCLUSIONS

In this paper, a cellular automaton model without step back for pedestrian movement in a channel considering the surrounding environment is presented. In this model, a pedestrian collects information about around cells before he makes his route choice. A parameter called interaction radius (R_i) is added to represent the range of around cells taken into account. Two groups of pedestrians are involved in the system: right walkers going from the left-hand boundary to the right-hand boundary, and left walkers going from the right-hand boundary to the left-hand boundary. It is found that the consideration of the surrounding environment is helpful and valuable to an efficient movement. It helps pedestrians to lower the probability of getting stuck. Movements with different system sizes have also been studied. The jamming transition does not depend on the system size, especially when the interaction radius value is large. Nonsymmetrical entrance densities on both boundaries are checked. The deviation of p_l and p_r plays a more important role at the early jamming state of pedestrian flow than at the free moving state. A new strategy is used to distinguish the influence of different pedestrian groups and results are compared with those derived before. It is shown that the new strategy improves the mean velocity but not the occupancy. Our model is represented as a basic frame model considering the surrounding environment. It can be extended by modifying simulation rules such as L and O functions to consider more complex situations in pedestrian flow in detail.

ACKNOWLEDGMENT

This work is supported by the National Natural Science Foundation of China Grant No. 50678164.

[1] C. Burstedde, K. Klauck, A. Schadschneider, and J. Zittartz, Physica A **295**, 507 (2001).

[2] A. Kirchner and A. Schadschneider, Physica A **312**, 260 (2002).

[3] A. Kirchner, K. Nishinari, and A. Schadschneider, Phys. Rev. E **67**, 056122 (2003).

[4] C. M. Henein and T. White, Lect. Notes Comput. Sci. **3415**, 173 (2005).

[5] W. G. Song, Y. F. Yu, B. H. Wang, and W. C. Fan, Physica A **371**, 658 (2006).

[6] D. Helbing, J. Keltsch, and Peter Molnar, Nature (London) **388**, 47 (1997).

[7] D. Helbing, A. Johansson, J. Mathiesen, M. H. Jensen, and A. Hansen, Phys. Rev. Lett. **97**, 168001 (2006).
[8] M. Muramatsu, T. Irie, and T. Nagatani, Physica A **267**, 487 (1999).
[9] K. Takimoto, Y. Tajima, and T. Nagatani, Physica A **308**, 460 (2002).
[10] W. F. Fang, L. Z. Yang, and W. C. Fan, Physica A **321**, 633 (2003).
[11] R. Nagai, M. Fukamachi, and T. Nagatani, Physica A **358**, 516 (2005).
[12] R. Nagai and T. Nagatani, Physica A **366**, 503 (2006).
[13] W. G. Weng, T. Chen, H. Y. Yuan, and W. C. Fan, Phys. Rev. E **74**, 036102 (2006).
[14] A. Kirchner, H. Klupfel, K. Nishinari, A. Schadschneider, and M. Schreckenberg, J. Stat. Mech.: Theory Exp. 2004, P10011.
[15] D. Helbing and P. Molnar, Phys. Rev. E **51**, 4282 (1995).
[16] D. Helbing, I. Farkas, and T. Vicsek, Nature (London) **407**, 487 (2000).